Effect of Air Lubrication on the Hydrodynamic Forces and Moments of KVLCC2 in Shallow Water

Gokula krishnan[1], Evgeni Milanov[2], Vijayakumar R[1]

[1]Department of Ocean Engineering, Indian Institute of Technology, Madras. Chennai, India.
[2]Bulgarian Ship Hydrodynamics Centre, Bulgarian Academy of Sciences, Varna, Bulgaria.

ABSTRACT

The use of air lubrication technology on ships has been advocated as a technique for reducing hydrodynamic drag and enhancing the operational efficacy of vessels. However, the potential advantages of air lubrication in situations with shallow water have not been thoroughly investigated. This research intends to determine the effect of air lubrication on the hydrodynamic forces and moment experienced by a KVLCC2 vessel during manoeuvres in shallow water. To accomplish this objective, a series of experiments were undertaken to utilise a 1:45.714 scale model of a KVLCC2 vessel in a towing tank facility at BSHC. The test of the appended hull model is compared to the virtual towing tank test. The numerical model based on the RANS equation was equipped with an air lubrication system and tested in shallow water. The model's hydrodynamic forces and moment were measured and compared to a control scenario devoid of air lubrication. The research revealed that the use of air lubrication on a KVLCC2 vessel in shallow water greatly decreases hydrodynamic forces and moments, resulting in enhanced manoeuvrability and overall operational efficiency. Specifically, air lubrication decreased the lateral force and yaw moment experienced by the model by up to 19%. In conclusion, this study reveals that air lubrication has the potential to reduce hydrodynamic forces and enhance manoeuvrability in shallow water. This study's results may be used to guide the design and operation of KVLCC2 and other vessel types in shallow water.

KEYWORDS: Air lubrication, hydrodynamic forces, manoeuvring, KVLCC2, shallow water

INTRODUCTION

The shipping industry plays a vital role in global commerce and is responsible for transporting a significant portion of the world's goods. However, the operation of ships is a major contributor to greenhouse gas emissions and energy consumption. One of the ways to reduce the environmental impact and increase the efficiency of ships is by reducing the hydrodynamic drag experienced by the vessel. One of the ways to do this is by using air lubrication technology (Jebin Samuvel et al., 2022)(Jebin Samuvel et al., 2022).

(Sindagi & Vijayakumar, 2020) (Sindagi & Vijayakumar, 2020) Air lubrication is a relatively new technology that involves the injection of air bubbles at the ship's hull to form a thin air film that separates the hull from the water. This air film can significantly reduce the friction between the hull and the water, leading to a reduction in hydrodynamic drag and an increase in the efficiency of vessel operations. However, air lubrication technology is still in the early stages of development, and more research is needed to fully understand its potential benefits and limitations when it comes to shallow water manoeuvring. Some of the challenges that need to be addressed include the design and maintenance of air lubrication systems and the environmental impact of injecting large amounts of air into the water (Sindagi et al., 2021)(Sindagi et al., 2021). Despite these challenges, the potential benefits of air lubrication make it a promising technology for improving the manoeuvrability of ships in shallow water environments.

One of the key factors that can affect the manoeuvring characteristics of a ship in shallow water is the ship's speed.(Feng et al., 2021) (Feng et al., 2021) The amount of air that enters under the hull of a ship is influenced by its speed, and this can have a notable impact on the ship's performance. As the ship moves at higher speeds, a greater amount of air can enter the system, resulting in a more significant decrease in frictional resistance. However, at lower speeds, the amount of air that can be entrained into the system may be more limited, resulting in a smaller reduction in frictional resistance. In addition, the angle of attack, or the angle at which the ship is moving through the water, can also affect the manoeuvring characteristics of a ship in shallow water. (Mucha et al., 2019) (Mucha et al., 2017) (Mucha et al., 2019) (Mucha et al., 2019) (Mucha et al., 2017)(Mucha et al., 2019) The angle of attack can affect the amount of air that is entrained into the system, which can have a significant impact on the ship's performance.

Overall, the use of air lubrication systems can have a significant impact on the manoeuvring characteristics of ships in shallow water environments (Foeth, 2008)(Foeth, 2008). The speed, draft, and angle of attack of the ship can all affect the performance of the air lubrication system, which can in turn affect the ship's manoeuvring characteristics. Further research is needed to better understand the complex interactions between air lubrication systems and the shallow water environment(Gokulakrishnan et al., 2022)(Gokulakrishnan et al., 2022), to optimize the performance of these systems in these challenging environments.

The present study aims to investigate the impact of air lubrication on the hydrodynamic forces and moment experienced by a well-researched KVLCC2 (KRISO Very Large Crude Carrier) during

manoeuvres in shallow water. The typical horizontal planar motion mechanism tests were performed for the KVLCC2 vessel to identify the hydrodynamic derivatives. A four-bladed E series propeller and a NACA 0018 semi-balanced rudder are used as the model's appendages. The experiments were conducted for a 7 m scale model without the air lubrication system in a 200 m long, 16 m wide, and 1.5 m deep shallow water towing tank at the Bulgarian Ship Hydrodynamic Centre.

Additionally, computational fluid dynamics studies are performed to determine the hydrodynamic behaviour of the KVLCC2 equipped with and without the air lubrication system using a RANS equation-based solver (Y. Liu et al., 2018)(Y. Liu et al., 2018). A standard k-ω SST turbulence model is employed for the numerical study. (I.T.T.C., 2017; H. Kim et al., 2015; Tiwari et al., 2020)(I.T.T.C., 2017; H. Kim et al., 2015; Tiwari et al., 2020) The free-surface refined hexahedral cells were employed to conduct the ITTC-recommended numerical test inside the computational domain (ITTC 2021). The Convergence study has been done to address the uncertainty in the time, iteration and grids in the numerical simulation. In this study, the required body motions have been modelled employing the overset mesh technique with three motion modes (pure sway, pure yaw, and combined sway and yaw motions). The tests were performed for the water depth to draft ratio (h/T=1.2), different flow rates (0.5 and 3 CFM - Cubic Feet per Minute) and various diameters of the holes (1 and 2 mm) of the scaled model of KVLCC2.

COORDINATE SYSTEM AND PRINCIPAL PARTICULARS OF KVLCC2

This study employs right-handed coordinate systems, as seen in Fig. 1. The ship's trajectory and direction are described in the coordinate system O_0 -x_0 y_0 z_0, where the x_0 -y_0 plane is fixed on the surface of still water and the z_0 axis points vertically downwards. The ship's hydrodynamic forces are modelled using a ship-fixed coordinate system O-XYZ, with the origin at mid-ship. The x-axis is oriented toward the bow, the y-axis is oriented toward the starboard, and the z-axis is oriented vertically downwards. The ship's centre of gravity is situated at (X_G, 0, 0). The heading angle is Ψ, the rudder angle is δ, and the yaw rate is r. The surge velocity and sway velocity are denoted by u and v, respectively. The drift angle at midship is defined as $\beta = \tan^{-1}(-v/u)$, and the overall velocity $U = \sqrt{u^2 + v^2}$. The principal particulars and test conditions are shown in Table 1.

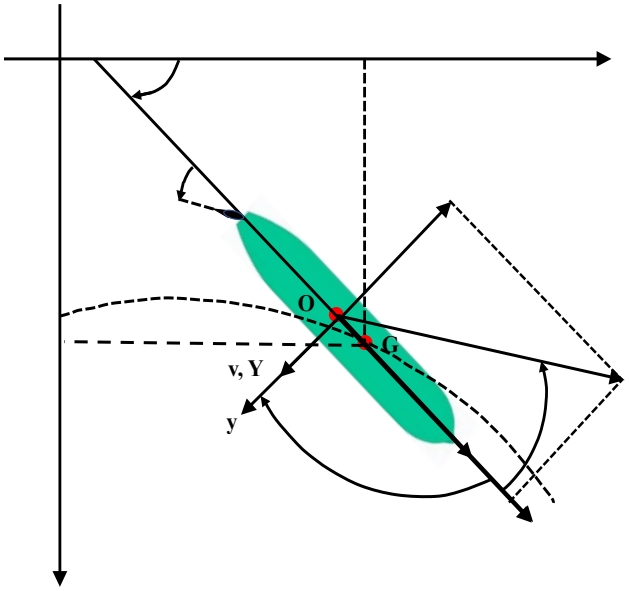

Fig. 1 Co-ordinate system used for studying the manoeuvring characteristics of KVLCC2.

Table 1: KVLCC2 hull, propeller, Rudder particulars and test conditions

KVLCC2	Prototype	(BSHC) Model
Scale	1	45.714
L_{bp} (m)	320	7
L_{wl} (m)	325.5	7.1204
B_{wl} (m)	580	1.2687
D (m)	30	0.6563
T (m)	20.8	0.455
Displacement (m^3)	312622	3.2724
S w/o rudder (m^2)	27194	13.0129
C_B	0.8098	
C_M	0.998	
LCB (%) fwd+	3.48	
Type	Horn	
S of the rudder (m^2)	273.3	0.1308
Lat. area (m^2)	136.7	0.0654
Turn rate (deg/s)	2.34	15.8
Propeller		
Type	FP	
No. of Blades	4	
D (m)	9.86	0.204
P/D (0.7R)	0.721	
Ae/A_0	0.431	
Rotation	Right hand	
Hub ratio	0.165	
Nominal revs. N0 (RPM)	(*)	
Test condition		
S (m2) incl. rudder	27467	13.144
LCG (m)	11.1	0.244
GM (m)	5.71	0.125
i_{xx}/B	0.4	
i_{zz}/Lbp	0.25	
U (m/s, full scale: kn)	7	0.532
Design Fn	0.064	0.064
h/T	1.2	
UKC (%)	20	
Water depth	24.96	0.546
Depth F_n	0.23	0.23

(*) at every water depth, the RPM is set as the model self-propulsion point at nominal speed U_0.

DESCRIPTION OF TESTS

Experimental Setup

The static and dynamic captive model experiments on Planar Motion Mechanism (PMM) were conducted in the BSHC Shallow Water Towing Tank. To produce stable and consistent results at lower h/T values, appropriate tank bottom flatness was required. This was accomplished by doing exact preparatory repairs, resulting in a bottom flatness of less than 10% of the model water depth-to draft ratio of h/T = 1.2. The PMM experiments were done employing the "Large amplitude horizontal planar motion mechanism" (LAHPMM) manufactured by Hydronautics Inc. and accessible at BSHC. Fig. 2 is a schematic representation of the model shown in the bow and aft region. Experiments were conducted for KVCC2 1:45.714 scaled model attached with NACA 0018 rudder and E series 4 bladed propeller at its self-propulsion point.

During all testing, the ship model was allowed to trim and heave but constrained in its ability to roll. Cuboid-shaped single-component

force load cells were used to measure drag force, yaw moment, and sway force. Motion kinematics, including bow and stern sinkage, were recorded. The ship-fixed coordinate system, commonly applied in PMM manoeuvring experiments, with the origin fixed at the COG of the model, was utilized for prescribing the motion characteristics and data collecting. Fig. 3 depicts a view of the KVLCC2 model attached to the PMM unit in the towing tank.

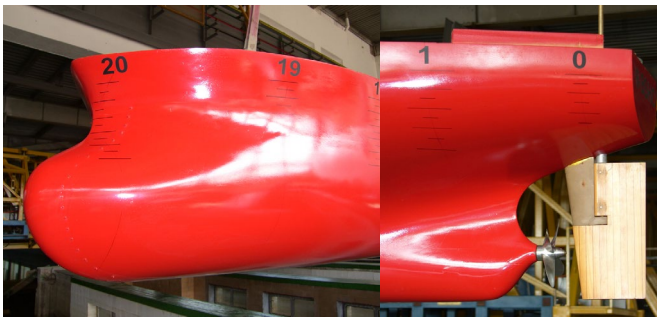

Fig. 2 Bow and aft of the KVLCC2 attached with NACA0018 rudder and E series four-bladed propeller

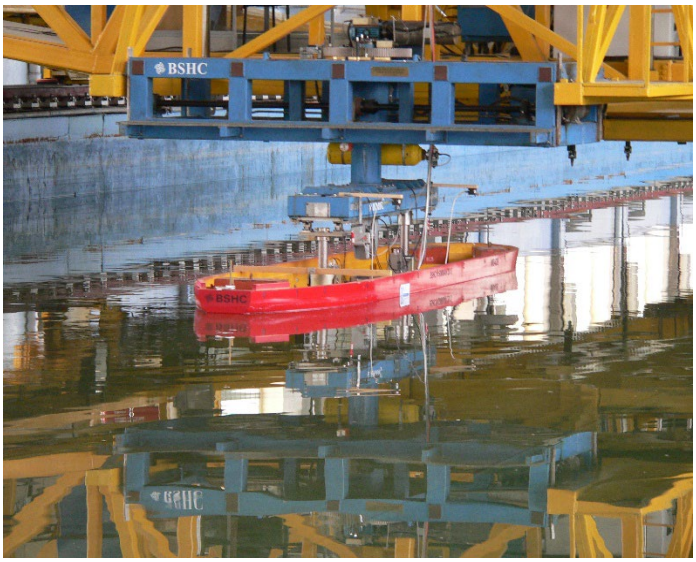

Fig.3 KVLCC2 mounted with PMM test setup in shallow water towing tank

Test conditions

The current investigation involves conducting captive model tests on KVLCC2 to examine its manoeuvring characteristics using experimental and computational fluid dynamic (CFD) techniques. To validate the reliability of the estimation of manoeuvring characteristics in shallow waters, the initial hull was examined without altering for the air lubrication system. However, for the CFD analysis, alterations were performed on the by introducing holes of varying diameters near the bow of the model to accommodate various flow rates as shown in Table 2.

The resistance and static drift test case was performed for both experiment and CFD. The effectiveness of the air lubrication is initially tested for a maximum drift angle of 10 degrees for all the numerical analyses. The dynamic Planar Motion Mechanism test was executed by both experiment and numerical studies. The PMM test consists of pure sway mode, pure yaw mode and combined sway and yaw modes. This is done by a sinusoidal oscillatory motion of the ship by an oscillatory frequency of 0.5 Hz. The maximum amplitudes are varied for different test conditions.

Table 2: Test Matrix of the KVLCC2 for the current study.

Parameters	Static Mode		Dynamic Mode (PMM Test)		
	Resistance Test	Drift Test	Pure Sway	Pure Yaw	Combined Yaw & drift
U (m/s)	0.2, 0.4, 0.532, 0.6	0.532	0.532	0.532	0.532
Oscillation frequency, f (Hz)	-	-	0.05	0.05	0.05
Max. Amplitude (m)	-	-	0.0677 0.1355 0.2032	0.0410 0.0819 0.1639	0.0410 0.0819 0.1639
Drift angle, β (deg)	-	-20,-10,-4,0,4,10,20	-	-	4
Diameter of the holes	1mm and 2mm (CFD)				
Flow rate	1.5 and 3 CFM (CFD)				

The main parameters of BSHC PMM during dynamic tests are shown in Eqn. 1, 2 and 3.
The sway velocity (v) can be expressed as

$$v = \dot{y} = -\omega y_m \cos(\omega t) = -v_m \cos(\omega t);\ \omega = 2\pi f \quad (1)$$

The course angle (ψ) & yaw velocity (r)

$$\psi = arctg[\frac{-\omega y_m}{U_C}\cos(\omega t)] \approx -\frac{\omega y_m}{U_C}\cos(\omega t) \approx \psi_m \cos(\omega t) \quad (2)$$

$$r = -\psi_m \omega \sin(\omega t) \quad (3)$$

NUMERICAL METHOD

Computational domain and boundary conditions

This fluid domain in Fig. 4 was used to run static and dynamic simulations, where LOA denotes the ship's overall length. It displays the ship's heading and the fluid's flow direction. The boundary conditions of the shallow water domain are intake as velocity entrance, exit as pressure outlet, and slip wall conditions at the sides and top. The surface of the hull and the bottom is subject to no-slip wall conditions. The option for wave dampening is engaged on the sidewalls to prevent wave reflections. Table 3 displays the solver settings used for this study. The Volume of Fluid (VOF) model considers the free surface impact at the air-water interface. As a flow solution, a three-dimensional segregated and Implicit Unsteady solver equation is used. In 0.01 seconds, the controlling equations were resolved.

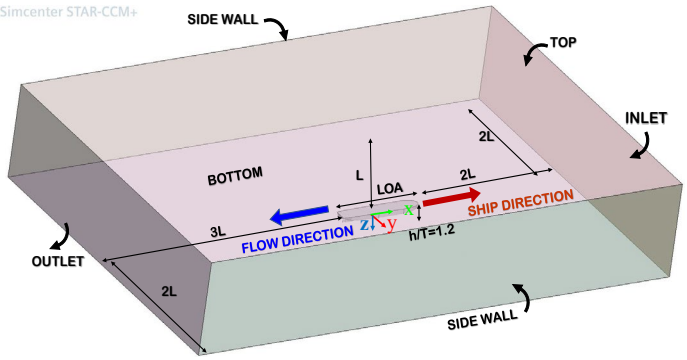

Fig. 4 Computational domain and boundary conditions used for the RANS equation-based solver.

Table 3: Solver parameters used for the CFD simulation.

Physical Parameters	Solver Settings
Solver	3D Segregated, Implicit Unsteady.
Turbulence Model	SST (Mentor) k-ω
Pressure discretisation	Standard
Wall treatment	All wall Y+
Momentum discretisation	Second-order upwind
Time discretisation	
Pressure-Velocity coupling	SIMPLE
Free surface modelling	The Volume of Fluid (VOF)
Y+ value	~1

Uncertainty studies

The grid convergence analysis was carried out for three meshes fine, medium, and coarse meshes. According to Richardson (1911), Grid Convergence research is required to estimate the uncertainty in the mesh, and the CFD findings have no impact on it. Roache (2008) provides a thorough approach for assessing the uncertainty in CFD applications owing to discretisation. The uncertainty analysis for the CFD investigation is shown in Table 4. The uncertainties for N1, N2, and N3 are computed (fine, medium, and coarse grids). Fine grid cells are 16.0 (10^6) in size, medium grid cells are 7.27 (10^6), and coarse grid cells are 3.31 in size (10^6). A convergence investigation was carried out for the various hydrodynamic derivatives (X', Y', N'). The following formula calculates the average gird size:

$$h = \left[\frac{1}{N}\sum_{i=1}^{N}(\Delta V_i)\right]^{1/3} \quad (4)$$

Where, ΔV_i = volume of the i^{th} cell, the following expression shows the apparent order (p)

$$p = \frac{1}{\ln(r_{21})}\left|\ln\left|\frac{\varepsilon_{32}}{\varepsilon_{21}}\right| + q(p)\right| \quad (5)$$

$$q(p) = \ln\left(\frac{r_{21}^{p} - s}{r_{32}^{p} - s}\right) \quad (6)$$

$$s = 1.sgn\left(\frac{\varepsilon_{32}}{\varepsilon_{21}}\right) \quad (7)$$

Where, $\varepsilon_{21} = \varphi_2 - \varphi_1$, $\varepsilon_{32} = \varphi_3 - \varphi_2$, q(p)=0, when $r_{21} = r_{32}$, sgn is the signal function.

$$sgn = \begin{cases} -1 & \text{if } \varepsilon_{21}/\varepsilon_{32} < 0 \\ 0 & \text{if } \varepsilon_{21}/\varepsilon_{32} = 0 \\ 1 & \text{if } \varepsilon_{21}/\varepsilon_{32} > 0 \end{cases} \quad (8)$$

$$e_a^{21} = \left|\frac{\phi_1 - \phi_2}{\phi_1}\right|, e_a^{32} = \left|\frac{\phi_2 - \phi_3}{\phi_2}\right| \quad (9)$$

$$\phi_{ext}^{21} = \frac{(r_{21}^{p}\phi_1 - \phi_2)}{(r_{21}^{p} - 1)}, \phi_{ext}^{32} = \frac{(r_{21}^{p}\phi_2 - \phi_3)}{(r_{32}^{p} - 1)} \quad (10)$$

$$e_{ext}^{21} = \left|\frac{\phi_{ext}^{12} - \phi_1}{\phi_{ext}^{12}}\right|, e_{ext}^{21} = \left|\frac{\phi_{ext}^{23} - \phi_2}{\phi_{ext}^{23}}\right| \quad (11)$$

The grid convergence index is

$$GCI_{fine}^{21} = \frac{1.25\, e_a^{21}}{r_{21}^{p} - 1} GCI_{fine}^{32} = \frac{1.25\, e_a^{32}}{r_{32}^{p} - 1} \quad (12)$$

The following relations are used to non-dimension forces [N], moment [Nm], Sway velocity_(v) [m/s] and Yaw velocity_(r) [deg/s]

$$X' = \frac{X}{0.5\rho L_{bp}{}^2 U^2} \quad (13)$$

$$Y' = \frac{Y}{0.5\rho L_{bp}{}^2 U^2} \quad (14)$$

$$N' = \frac{N}{0.5\rho L_{bp}{}^3 U^2} \quad (15)$$

$$v' = \frac{v}{U_0} \quad (15)$$

$$r' = \frac{r.L}{U_0} \quad (16)$$

Table 4: Uncertainty analysis of KVLCC2 in shallow water h/T=1.2 for the drift angle β=4°

Non-dimensional hydrodynamic forces and moment		X'	Y'	N'
Number of cells (10^6)	Fine, Medium, Coarse	16.0, 7.27, 3.31		
Average grid size	h_1, h_2, h_3	0.1297, 0.1686, 0.2192		
Grid refinement factor	r_{21}, r_{32}	1.3, 1.3		
Non dimensional Hydrodynamic forces and moments for different grids	Φ_1, Φ_2, Φ_3	0.000168, 0.000165, 0.000162	0.00644, 0.00597, 0.00566	0.00230, 0.00211, 0.00196
Apparent order	p	1.0965	1.7914	0.9579
Approximate relative error (%)	e_a^{21}, e_a^{32}	1.48, 2.0	7.41, 5.00	8.26, 7.00
Extrapolated values	φ_{ext}^{21}, φ_{ext}^{32}	0.000175, 0.00018	0.00724, 0.00646	0.00297, 0.00263
Extrapolated relative error (%)	e_{ext}^{21}, e_{ext}^{32}	4.25, 5.64	10.99, 7.66	22.42, 19.61
GCI (%)	GCI_{fine}^{21}, GCI_{fine}^{32}	5.54, 7.47	15.43, 10.37	36.12, 30.49

Eqn.4-16 explains the procedure to determine the uncertainties present in the numerical grids. This method is widely used for verifying the numerical simulation without validation study for various computational problems.

The analysis reveals that altering the using various cell-size grids does not affect the solution. The computational cost of finding a solution for the finer grid is too expensive. This uncertainty analysis is required for each CFD study to save computing time. As a consequence, medium meshing was selected for further numerical analysis. The drag force X' is 5.54% for GCI fine21 and 7.47% for GCI fine32, indicating that the medium is acceptable for investigating drag force and that the convergence is monotonic. The yaw moment and the sway force are also in monotonic convergence. As a result, the medium grid is selected for further studies as shown in Fig. 5.

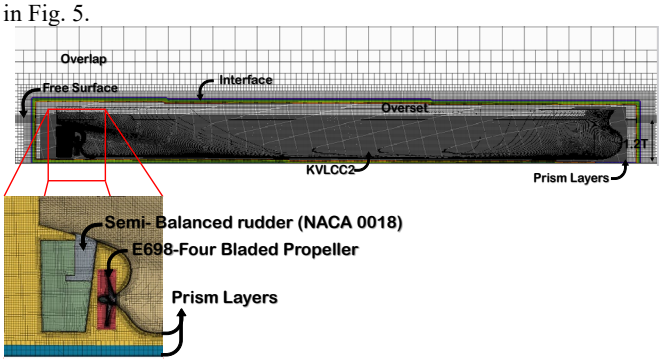

Fig. 5 Mesh refinement of KVLCC2 for h/T=1.2

Validation for the manoeuvring studies

The validation of the numerical analysis is done by comparing the experimental test results from BSHC and the INSEAN experimental result provided by the SIMMAN, Workshop on Verification and Validation of Ship Manoeuvring Simulation Methods. (J. Liu et al., 2015; Toxopeus, 2013; J. Liu et al., 2015; Toxopeus, 2013; Jebin Samuvel, 2022) The relative error is found to be less than 5 % for all the computational simulations. Over the years computational fluid dynamic software packages like Starccm+, and Open foam predicts the hydrodynamic behaviours very efficiently for ship manoeuvrability simulations. Fig. 6-8 represents the comparison of surge force, sway force and yaw moment for the different drift angle, sway velocity and yaw velocity of KVLCC2 for the h/T = 1.2. This water depth is called an extreme shallow water case.

The hydrodynamic force X' shows the non-dimensional surge force which majorly depends on the drag or resistance of the ship. This has a lesser impact on the manoeuvring performance of the ship. The hydrodynamic sway force Y' and hydrodynamic yaw moment N' which are majorly contributing to the turning characteristics of the vessel. Fig. 6-8 clearly shows the sway force and yaw moment are dominant.

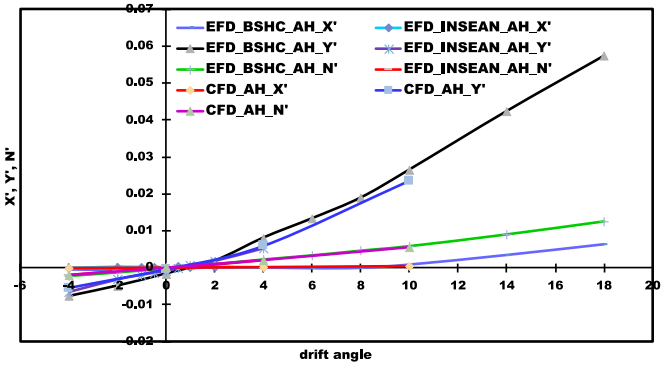

Fig. 6 Non-dimensional surge force, sway force and yaw moment against the drift angle of appended KVLCC2

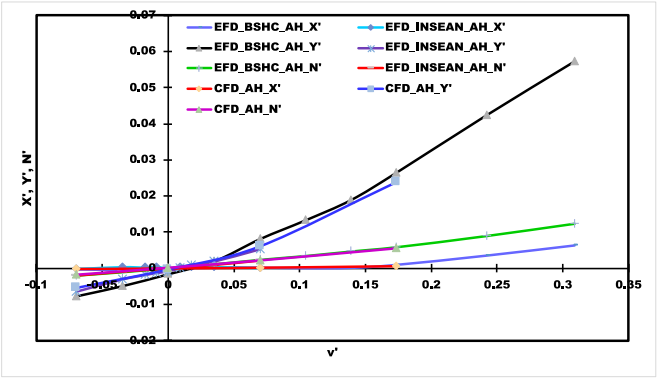

Fig. 7 Non-dimensional surge force, sway force and yaw moment against the sway velocity of KVLCC2

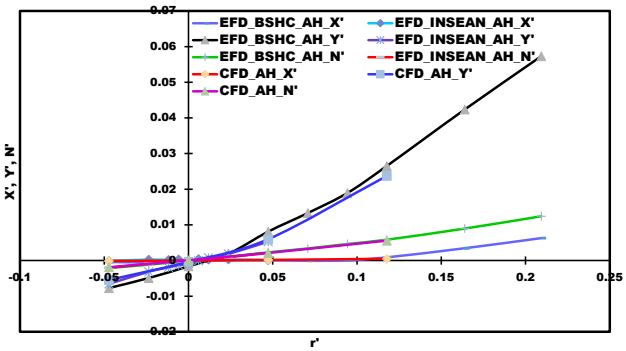

Fig. 8 Non-dimensional surge force, sway force and yaw moment against the angular velocity of KVLCC2

Validation for the air lubrication studies.

An experiment carried out by (Moriguchi & Kato, 2002) was used to validate the numerical method for the flat plate with and without air lubrication as shown in Fig. 9. To confirm the frictional resistance, the shear stress of the channel was first measured without air injection. Simulations were then conducted at speeds ranging from 4m/s to 8m/s in 1m/s intervals. The shear stress results were compared with experimental results, with and without air injection, at two locations 750mm and 1250mm from the point of injection. Furthermore, simulations were conducted to study the effect of air injection rates on frictional drag reduction at a speed of 5m/s.

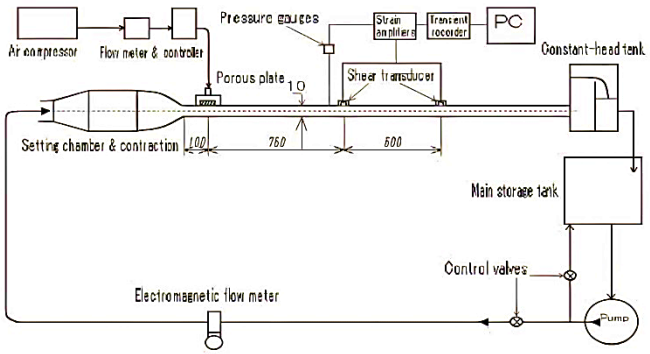

Fig. 9 Experimental setup used by Moriguchi & Kato, 2002 to study the effect of air lubrication.

In the numerical setup, air was injected through a series of 1mm diameter holes in the upstream upper surface of the test section to generate air-liquid flow. The friction and void fraction values were measured and compared to experimental results at 750mm from the air injection point at one transverse position to determine their effect on the frictional coefficient. Fig. 9 shows a comparison between the

frictional resistance coefficient obtained from the experiment and simulation without air injection. Eqn. 17 and 18 represent the mean velocity (U_m) and frictional coefficient (C_f), respectively.

$$U_m = \frac{Q_a + Q_w}{b.h} \tag{17}$$

$$C_f = \frac{\tau_w}{0.5.\rho_m.U_m^2} \tag{18}$$

Where Q_a–air injection rate, Q_w–water flow rate, b–breath of the domain, h – height of the test section, τ_w–shear stress, ρ_m–mean density,

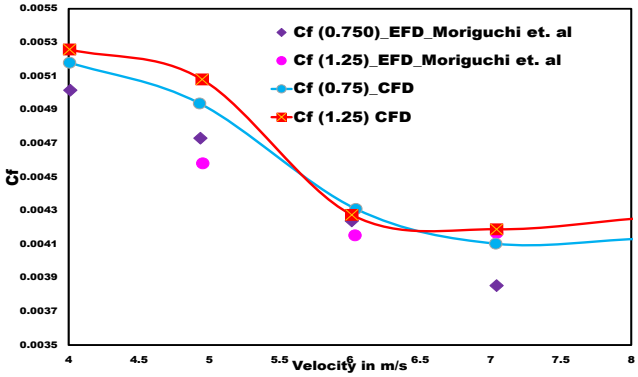

Fig. 10 Comparison of the friction coefficient (C_f) with experimental results was done in the absence of air injection.

The comparison between the results of frictional resistance reduction obtained from the experiment and simulation with and without air injection is shown in Fig. 10. Simulations were carried out at a speed of 5m/s with ten different air injection rates. Eqn. 19 pertains to the void fraction or volume fraction (α_m).

$$\alpha_m = \frac{Q_a}{Q_a + Q_w} \tag{19}$$

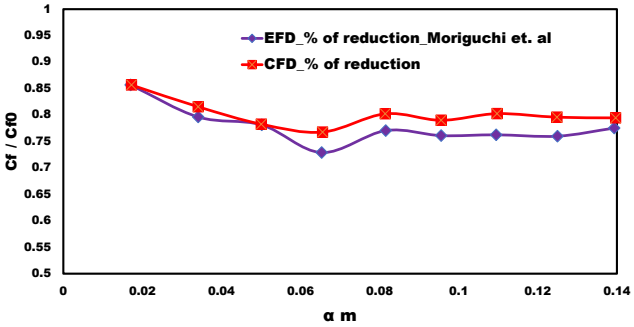

Fig. 11 Comparison of the percentage of reduction in friction coefficient (C_f) with experimental results with the air injection.

The results obtained from the comparison between simulation and experimental data by Moriguchi & Kato, 2002 indicate a strong agreement between the two sets of findings. Specifically, the simulation outcomes closely resemble the experimental results, demonstrating the accuracy and effectiveness of the simulation model. Moreover, injecting air beneath the plate leads to a significant reduction in the amount of frictional drag, which is a major contributor to energy loss and inefficiency in fluid flow systems.

The magnitude of the reduction achieved through air injection is dependent on several factors, including the percentage of voids in the fluid, the speed of the flow, and the distance between the injection point and the analysis location. These variables can impact the effectiveness of air injection and the degree to which it can mitigate frictional drag. Therefore, it is crucial to consider these factors when designing fluid flow systems with the aim of reducing energy loss and improving efficiency.

Based on the data analysed, the highest reduction in frictional drag achieved through air lubrication is 33% for a flat plate, which aligns with the results obtained from experiments. This finding underscores the potential of air lubrication as a strategy for improving the efficiency of fluid flow systems. By reducing the amount of energy loss due to frictional drag, air lubrication can lead to significant cost savings and environmental benefits.

The current investigation employs the identical CFD approach that was used in a prior study validating an air lubrication system. The objective is to examine how air lubrication affects the KVLCC2's operation in shallow water conditions. CFD simulations are a useful technique for obtaining a comprehensive understanding of the intricate fluid dynamics in play and revealing how the KVLCC2 behaves in different operating scenarios.

RESULTS AND DISCUSSIONS

The 7m KVLCC2 scaled model underwent a series of experimental and computational simulation tests. The experimental test results were analysed and compared with the CFD results and found that there was a notable agreement for the appended hull in the absence of air lubrication. This finding is significant because it suggests that the hull design plays a crucial role in ship hydrodynamics, particularly in terms of improving efficiency and reducing drag. The CFD shows as depicted in Figure 12, the KVLCC2 model was fitted with a rudder and propeller, and its under-keel velocity profile was measured. The results showed that the velocity near the bow of the under-hull was measured at 1.05 m/s, which is nearly twice the inflow velocity of the ship, 0.532 m/s. This observation is due to the SQUAT effect, which arises from the coupled sinkage and trim. The fluid velocity increases due to the reduction in the water depth, which induces a decrease in the pressure in that region. The decreased pressure then results in the SQUAT effect. It is worth noting that the SQUAT effect can cause a significant reduction in the available under-keel clearance, posing a potential risk for ship grounding. Therefore, understanding this phenomenon is crucial for the safe navigation of ships in shallow waters.

In the current study, a modified KVLCC2 is utilised to examine the impact of air lubrication, as depicted in Fig. 13. The modification was made in the keel area near the bow region of the vessel. To accomplish this, we utilized a perforated hull with #10 x #50 holes of varying diameters - 1mm and 2mm. Atmospheric air was induced through the holes in the form of a mass flow rate. We conducted further tests on the modified hull using various flow rates of 0.5 CFM and 3 CFM.

This modification allowed us to investigate the effectiveness of air lubrication in reducing frictional drag and improving fuel efficiency in ship operations. The use of perforated hulls with induced air flow has been demonstrated to reduce the resistance of a vessel in water, and hence lower the power required to propel the ship, resulting in significant fuel savings. By variation with different hole diameters and air flow rates, this study aim to understand the performance of air lubrication and identify the most effective configuration for future implementation in ship design and operation.

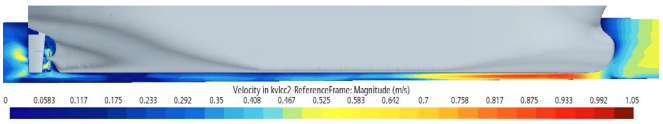

Fig. 12 Velocity profile of appended KVLCC2 for h/T=1.2, F_n=0.064

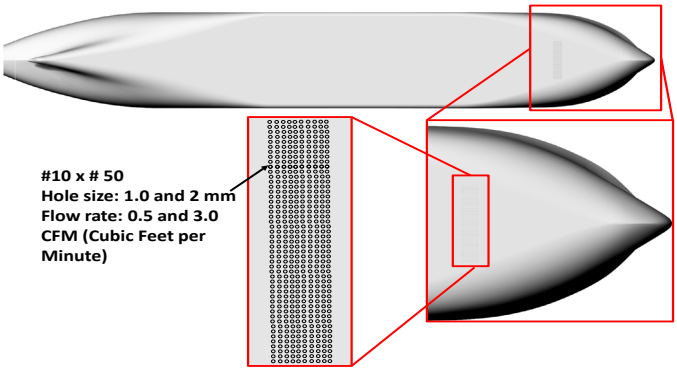

Fig. 13 Modified KVLCC2 hull for the air lubrication system

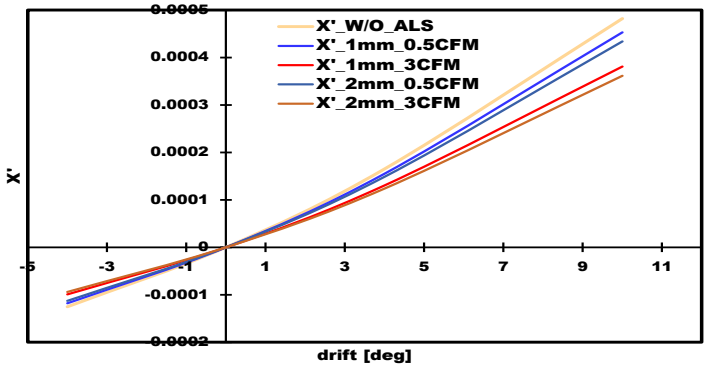

14 (a)

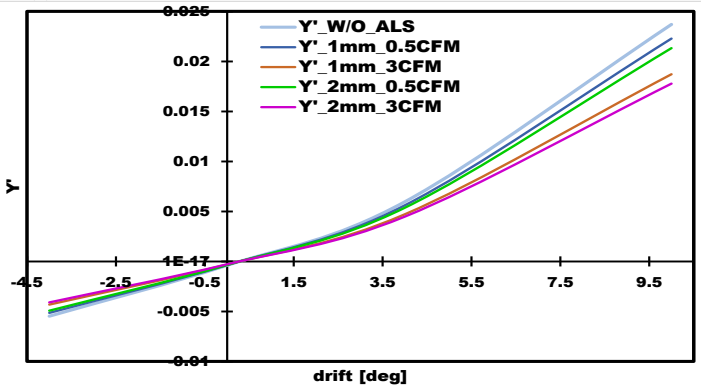

14 (b)

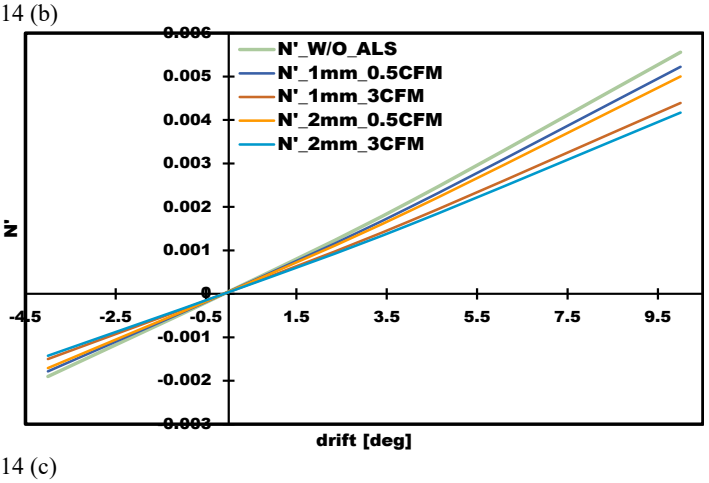

14 (c)

Fig. 14 Non-dimensional (a) surge force, (b) sway force and (c) yaw moment from static drift test of KVLCC2 without air lubrication and with 0.5 CFM and 3 CFM for 1mm and 2mm holes respectively.

Where W/O_ALS –without Air Lubrication system.

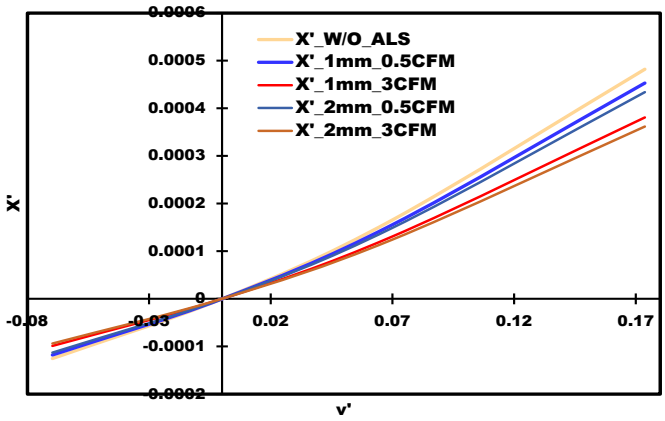

15 (a)

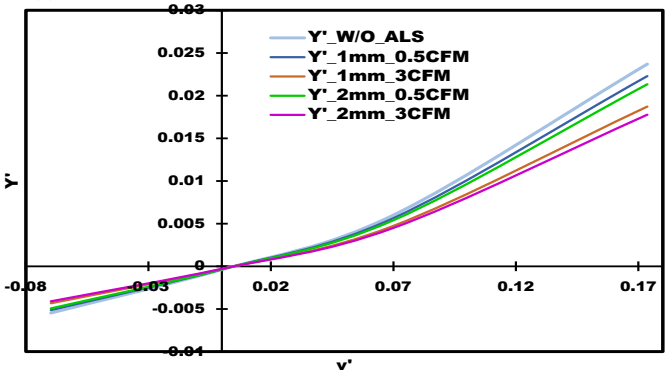

15 (b)

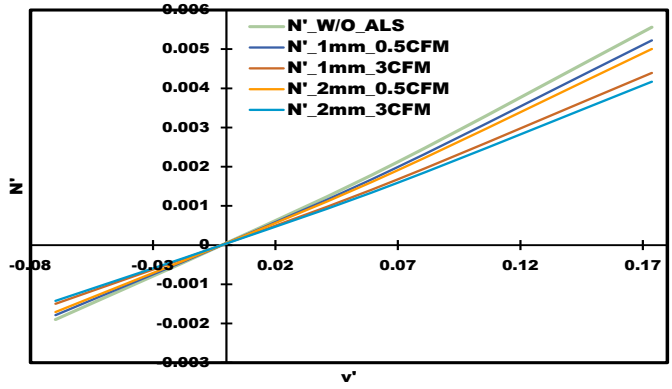

15 (c)

Fig. 15 Non-dimensional (a) surge force, (b) sway force and (c) yaw moment for different sway velocity of KVLCC2 without air lubrication and with 0.5 CFM and 3 CFM for 1mm and 2mm holes respectively.

The present study involves an analysis of the hydrodynamic behavior of the KVLCC2, with a focus on the effects of air lubrication on its manoeuvring aspects. The modified hull was used for further study, and its performance was compared with the unmodified hull used in validation for the manoeuvring studies. The captive model test was performed to understand the nondimensional surge force, sway force, and yaw moment acting on the hull. The results of the tests, conducted at different drift angles, sway velocities, and angular velocities, are shown in Figures 14, 15, and 17. The results indicate that the non-dimensional surge force X' is significantly smaller than the non-dimensional sway force Y' and yaw moment N'. The Y' is found to be ten times larger than the X'. For the current study, the Y' and N' have a major contribution in understanding the effect of air lubrication on the manoeuvring aspects of KVLCC2.

The results show that air lubrication has a significant effect in reducing the non-dimensional surge force X', sway force Y', and yaw moment N'. The maximum reduction was identified for the 3

CFM in 2mm holes modified hull, which clearly indicates the effectiveness of air lubrication in reducing the hydrodynamic forces acting on the hull. The slope of the graph represents the hydrodynamic resistance of the ship, with a steeper slope indicating higher resistance and lower speed, which was found in the W/O_ALS. Slightly lower resistance was found for the 2mm_3CFM configuration, indicating the potential for improved manoeuvrability with air lubrication.

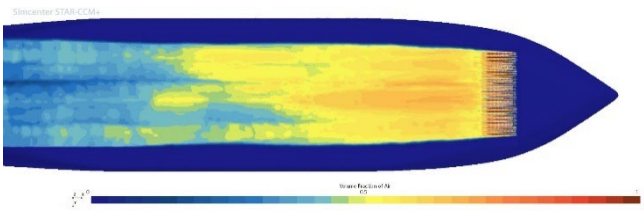

Fig. 16 Variation of volume fraction of air in the KVLCC2 hull

The changes in the volume fraction of air in the KVLCC2 hull are depicted in Figure 16, providing valuable insights into the real-world physics of air lubrication. The scalar view created allowed for the visualization of the air lubrication distribution on the hull, highlighting an increase in the volume fraction of air near the holes, which indicates that more air is being trapped and retained in these areas. Conversely, the volume fraction of air decreases towards the aft of the ship. This variation in the volume fraction of air has the potential to reduce frictional drag and improve the fuel efficiency of the vessel, particularly when it is operating at a drift angle of 0 degrees. Therefore, analysing the changes in the volume fraction of air in the KVLCC2 hull is crucial for understanding the effectiveness of the air lubrication system and optimizing its performance. This can be studied in the future research.

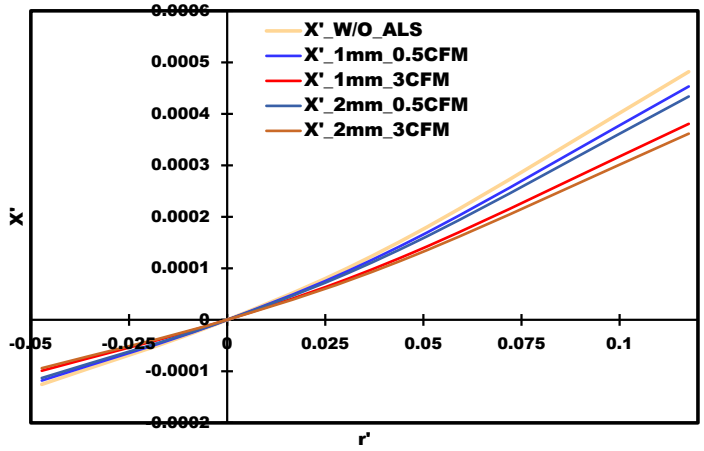

17 (a)

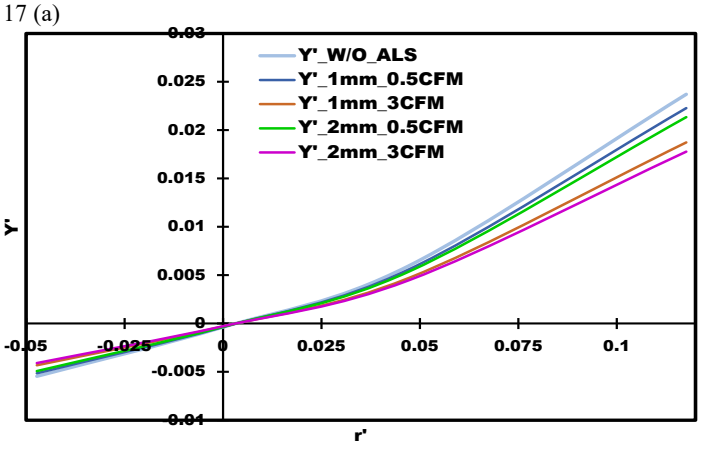

17 (b)

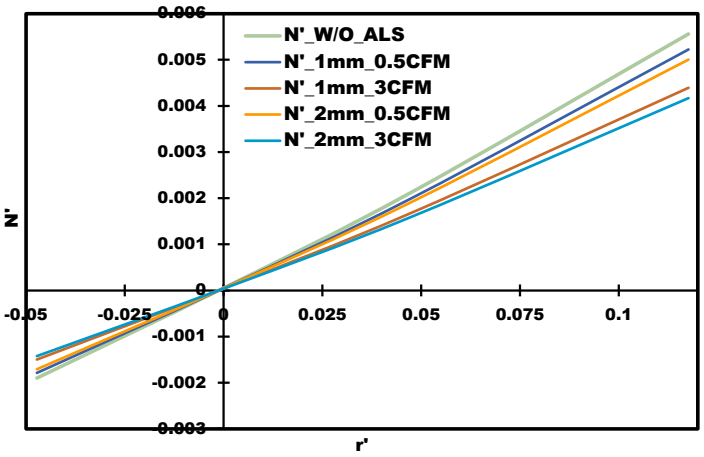

17(c)

Fig. 17 Non-dimensional (a) surge force, (b) sway force and (c) yaw moment for different angular velocity of KVLCC2 without air lubrication and with 0.5 CFM and 3 CFM for 1mm and 2mm holes respectively.

The present study has shed light on the significant role of air lubrication in enhancing the manoeuvrability of the KVLCC2 vessel, especially when navigating through shallow waters. The results have shown that the use of air lubrication technology can effectively reduce the hydrodynamic forces acting on the hull, which can lead to significant improvements in fuel efficiency and a reduction in operational costs.

The findings of this study highlight the potential of air lubrication technology to revolutionize the shipping industry, as it offers a practical solution to improve the performance of large vessels like the KVLCC2. The study has established that air lubrication technology can provide a cost-effective alternative to traditional anti-fouling coatings, which can be expensive and time-consuming to apply.

CONCLUSION AND FUTURE STUDIES

Conclusion

- A numerical captive model test has been performed for KVLCC2 using a RANS equation based CFD solver and has good agreement with the experimental test conducted by the Bulgarian Ship Hydrodynamics Centre, Bulgaria, with appendages.
- The air bubbles have been introduced in the forward of the hull, and the hydrodynamic characteristics are studied by varying the hole size of (1 mm and 2 mm) and the flow rates of (0.5 CFM and 3 CFM).
- A maximum of 19% reduction in sway force was found for 2mm holes with a 3CFM flow rate.
- This study has highlighted the potential of air lubrication technology in enhancing the manoeuvrability and reducing the operational costs of large vessels like the KVLCC2, particularly when navigating through shallow waters. The findings have significant implications for the shipping industry and offer new opportunities for the development of sustainable shipping practices.

Future studies

- To investigate its effect on turning circle, rudder angle, and stopping distance. Additionally, optimizing the air lubrication system for maximum performance and establishing guidelines for installation and maintenance on large vessels like the KVLCC2 are essential.

- To explore the impact of various parameters such as hole diameter, flow rate, and h/T ratio on frictional drag reduction.
- Conducting a sensitivity analysis of each hydrodynamic derivative could provide valuable insights into the effectiveness of air lubrication on reducing hydrodynamic forces.
- To determine the trajectories of modified vessels equipped with air lubrication systems to fully explore the technology's potential in enhancing the KVLCC2's manoeuvrability under different operating conditions.

ACKNOWLEDGEMENT

This study is supported in part by the International Immersion Experience program (IIT Madras), India. and by the Ministry of Human Resource Department, Government of India. The authors wish to acknowledge the Bulgarian Academy of Sciences, IMSET" ACAD.A.BALEVSKI" Bulgarian Ship Hydrodynamics Centre (BSHC), Bulgaria, High-Performance Computing Environment, IIT Madras India. and Department of Ocean Engineering, Indian Institute of Technology Madras, India.

REFERENCES

Feng, Y., el Moctar, O., & Schellin, T. E. (2021). Parametric Hull Form Optimization of Containerships for Minimum Resistance in Calm Water and in Waves. *Journal of Marine Science and Application*, *20*(4), 670–693. https://doi.org/10.1007/S11804-021-00243-W/FIGURES/30

Foeth, E. J. (2008). *20 th International Hiswa Symposium on Yacht Design and Yacht Construction Decreasing frictional resistance by air lubrication*.

Gokulakrishnan, G., Jebin Samuvel, T., Kumar, A., & Vijayakumar, R. (2022). Numerical prediction of hydrodynamic forces and moments of KCS in shallow water. *Oceans Conference Record (IEEE)*. https://doi.org/10.1109/OCEANSCHENNAI45887.2022.9775441

I.T.T.C. (2017). Guidelines on use of RANS tools for maneuverability prediction. ITTC Recommended Procedures and Guidelines 7.5-03-04-01. *Proceedings of 26th International Towing Tank Conference*.

Jebin Samuvel, T., Gokulakrishnan, M., Kumar, A., & Vijayakumar, R. (2022). Numerical Estimation of Frictional Drag on Flat Plate In Shallow Water with & without BDR. *Oceans Conference Record (IEEE)*. https://doi.org/10.1109/OCEANSCHENNAI45887.2022.9775316

Kim, H., Akimoto, H., & Islam, H. (2015). Estimation of hydrodynamic derivatives by RANS simulation of planar mechanism test. *Ocean Engineering*, *108*(2015), 129–139.

Kim, H. T., Kim, H. T., Kim, J. J., & Lee, D. Y. (2021). Study on the Skin-Friction Drag Reduction by Air Injection Using Computational Fluid Dynamics-Based Simulations. Lecture Notes in Civil Engineering, 63 LNCE, 205–226. https://doi.org/10.1007/978-981-15-4624-2_12

Liu, J., Hekkenberg, R., Rotteveel, E., & Hopman, H. (2015). Literature review on evaluation and prediction methods of inland vessel manoeuvrability. *Ocean Engineering*, *106*(2015), 458–471. https://doi.org/10.1016/j.oceaneng.2015.07.021

Liu, Y., Zou, L., Zou, Z., & Guoa, H. (2018). Predictions of ship maneuverability based on virtual captive model tests'. *Engineering Applications of Computational Fluid Mechanics*, *12*(1), 334–353. https://doi.org/10.1080/19942060.2018.1439773.

Moriguchi, Y., & Kato, H. (2002). Influence of microbubble diameter and distribution on frictional resistance reduction. In *Journal of Marine Science and Technology* (Vol. 7, Issue 2). https://doi.org/10.1007/s007730200015

Mucha, P., Dettmann, T., Ferrari, V., & el Moctar, O. (2019). Experimental investigation of free-running ship manoeuvers under extreme shallow water conditions. *Applied Ocean Research*, *83*, 155–162. https://doi.org/10.1016/J.APOR.2018.09.008

Mucha, P., el Moctar, O., Dettmann, T., & Tenzer, M. (2017). Inland waterway ship test case for resistance and propulsion prediction in shallow water. *Http://Dx.Doi.Org/10.1080/09377255.2017.1349723*, *64*(2),106–113. https://doi.org/10.1080/09377255.2017.1349723

Moriguchi, Y., & Kato, H. (2002). Influence of microbubble diameter and distribution on frictional resistance reduction. In Journal of Marine Science and Technology (Vol.7,Issue 2). https://doi.org/10.1007/s007730200015

Sindagi, S., & Vijayakumar, R. (2020). Succinct review of MBDR/BDR technique in reducing *ship's drag*. https://doi.org/10.1080/17445302.2020.1790296

Sindagi, S., Vijayakumar, R., & Saxena, B. K. (2021). Experimental parametric investigation to reduce drag of a scaled model of bulk carrier using BDR/ALS Technique. *Journal of Ship Research*, *65*(3), 257–265. https://doi.org/10.5957/JOSR.02190009

Tiwari, K., Hariharan, K., Rameesha, T., & Krishnankutty, P. (2020). Prediction of a research vessel manoeuvring using numerical pmm and free running tests. *Ocean Systems Engineering*, *10*(3), 333–357.

Toxopeus, S. L. (2013). Viscous-flow calculations for KVLCC2 in deep and shallow water. *Computational Methods in Applied Sciences*, *29*, 151–169. https://doi.org/10.1007/978-94-007-6143-8_9

Yoshimura, Y., Ueno, M., & Tsukada, Y. (2008). Analysis of Steady Hydrodaynamic Force Components and Prediction of Manoeuvering Ship Motion With Kvlcc1, Kvlcc2 and Kcs. *Proceedings of Workshop on Verification and Validation of Ship Manoeuvring Simulation Methods*, *4*.